CLIPPING CONTOURS: AN RFPA DESIGN TOOL

Tim Canning, Steve C. Cripps

Centre for High Frequency Engineering, Cardiff University, Cardiff, UK, CF24 3AA

Contact: canningt@cardiff.ac.uk

ABSTRACT

This paper presents the “clipping contour”, a new RFPA design tool which enables the designer to visualise and control the possibly detrimental effects of the second harmonic impedance, maintaining power, linearity and efficiency in broadband RFPA designs. This new tool allows the designer to prevent the voltage waveform from crossing zero, thus clipping the current waveform and degrading performance. This simplifies the process of managing waveform interaction with the device knee region, and expands the continuous mode design space to incorporate non-zero second harmonic resistive matching. A design example is fabricated, demonstrating the utility of the second harmonic clipping contour tool as part of the PA design process. A 10W GaN demonstrator gives measured CW power >8.5W, drain efficiency >60%, and better than -30dB ACPR over a bandwidth of 1-2.9GHz.

INTRODUCTION

RF power amplifiers (RFPAs) have, both historically and currently, been designed by attempting to realise various well-analysed modes, typically identified by a letter (A, B, C, D, E etc.), all of which have been the subject of extensive research [1-5]. These modes, however, define only singular impedance points in a multi-dimensional harmonic impedance space; the effect of a practical circuit response which inevitably ``misses" such a singular point in any of the harmonic dimensions has never historically been analysed [6]. This is a frustration for designers, where the task of realizing a practical circuit that meets the singular conditions of a particular PA mode over a range of frequencies is limited by theoretical as well as practical constraints.

This paper presents further analysis of the Class B/J continuous mode, part of continuous mode theory as described in previous work [7-11]. The resulting equations yield a useful new graphical tool called the “second harmonic clipping contour” [12].

Crucially, the clipping contour displays (for any given fundamental impedance, ZF0) the region of the smith chart where the second harmonic impedance (Z2F0) will not cause the voltage waveform to interact with the knee, i.e. have a global minimum voltage below the knee voltage. This new tool enables the designer to target a voltage waveform that will avoid efficiency (η), linearity and power degrading modulation of the current waveform.

In this work, a 10W GaN RFPA is presented which obeys the clipping contours condition over its operating bandwidth, maintaining high efficiency and linearity from 1-2.9GHz. Power and η is maintained over this almost 3:1 bandwidth as well as showing good initial linearity measurements.

THEORY

The waveform engineering process can be summarized concisely, inasmuch as the most efficient current waveform (at the current generator or "Igen" plane) is well defined and essentially ``universal", regardless of the particular device size, type or frequency [6][13]. The optimum current waveform is one which maximizes the in phase fundamental to DC harmonic ratio and hence, drain efficiency (η). This optimum waveform is a close approximation to a half-wave rectified sine wave, and is usually engineered at the input by un-biasing the device close to the pinch-off point, although at higher frequencies some additional harmonic tuning may be required [14].

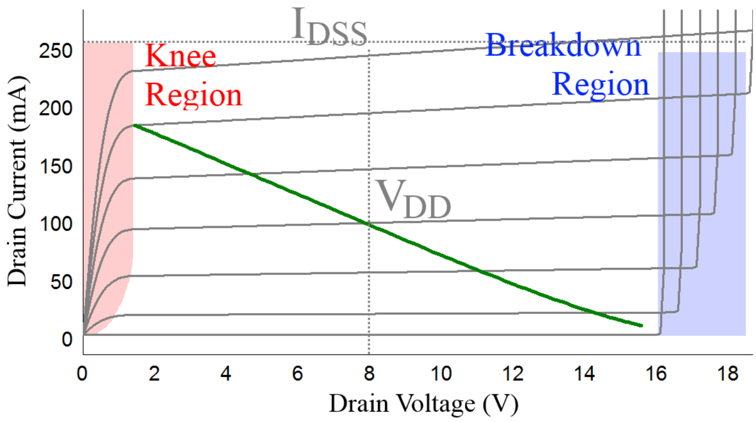

Figure 1: Typical transistor DCIV, highlighting the operating boundaries which the waveforms must not violate.

The design task therefore is constrained primarily to presenting the device Igen plane with a multi-harmonic impedance environment, so as to generate a voltage waveform. This voltage waveform must be both efficient (by maximising the fundamental to DC ratio), but also crucially which can be supported within the operating boundaries imposed by the technology. Figure 1 shows a typical transistor DCIV response, highlighting the four main device boundaries. For RFPAs targeting high efficiencies, the designer aims to avoid the top right section of the IV plot, corresponding to high levels of power dissipated in the device. Of *critical* importance therefore, is the interaction with the non-linear and hence performance degrading knee region, with which the waveform will interact closely.

Conventional RFPA modes typically specify only singular voltage waveforms (and hence singular impedance sets) for the designer to target. Continuous mode theory expands upon this by allowing these impedance sets to "move" along defined trajectories, permitting a compromise between reactance and peak voltage. These impedance trajectories are however rigidly defined, i.e. the theory gives no guidance as to the effect on performance if these targets are missed. This presents a problem to the RFPA designer, who is provided with matching elements, the impedances of which change significantly over frequency, making it difficult to adhere to these target trajectories. Additionally, the designer is left with no guide as to the sensitivity of these modes; if the targets will be missed, where should the impedances be located to minimise performance degradation?

$$V(\theta) = [1 - \cos(\theta + \delta)][1 + \beta \sin(\theta + \gamma)] \qquad \textbf{(1)}$$

Clipping contours address this problem by expanding the Class B/J voltage waveform to a general set (1) which "graze zero", that is, which possess a global minimum voltage value equal to zero. Any waveform containing DC, fundamental and second harmonic voltage, and critically, possessing a global minimum voltage of zero, can be described by (1).

$$v_{1r} = \frac{\beta \sin\gamma - \cos\delta}{1 - \frac{\beta}{2}\sin(\gamma - \delta)} \qquad v_{1q} = \frac{\beta \cos\gamma + \sin\delta}{1 - \frac{\beta}{2}\sin(\gamma - \delta)} \tag{2}$$

$$v_{2r} = \frac{-\frac{\beta}{2}\sin(\delta + \gamma)}{1 - \frac{\beta}{2}\sin(\gamma - \delta)} \qquad v_{2q} = \frac{-\frac{\beta}{2}\cos(\delta + \gamma)}{1 - \frac{\beta}{2}\sin(\gamma - \delta)}$$

Taking the Fourier series of (1) and normalising the coefficients to DC gives (2). Since the current waveform is "fixed", these voltages are *synonymous with impedances*. It is also important to note that, as v1r is normalised, both the power and efficiency are governed solely by this value. Fixing the fundamental impedance ZF0 and solving (2) for the second harmonic impedance Z2F0 yields a linear set of solutions for the Z2F0. These impedances we designate the "clipping contour".

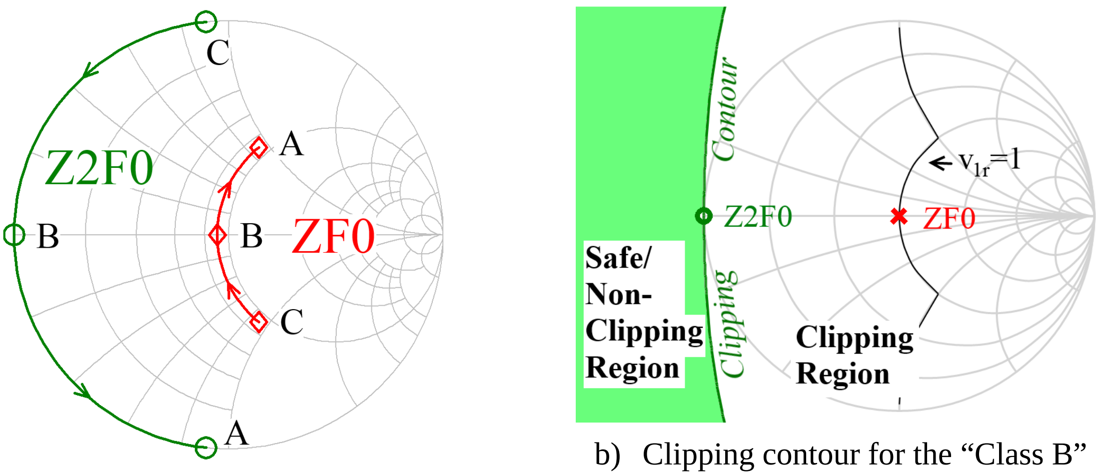

a) Class B/J showing singular pairs along the trajectory

b) Clipping contour for the "Class B" condition showing the extended non-clipping space.

Figure 2: Comparing Class B/J with the extended Clipping Contours trajectory.

Figure 2b shows an example of a clipping contour plotted when ZF0 is equal to the optimal load line impedance RL, given by (3).

$$RL = 2 * VDD/IDSS \tag{3}$$

Figure 2b represents the classical Class B condition, where the second and higher harmonic impedances are a short circuit. Usefully, as the voltage terms are normalised to DC, i.e. the DC value is always unity, the knee voltage can be changed from zero to any arbitrary value by applying a simple, linear scaling coefficient to all the harmonic voltage terms above DC.

The critical differences between both classical and continuous modes, and the new clipping contour tool are

1. The ability of the clipping contour to show the optimal (zero-grazing voltage waveform) Z2F0 impedances, for *any* ZF0, not restricted to a rigid trajectory (Figure 2a).
2. Identification of an optimal Z2F0 *region*, inside which the voltage waveform will have a global minimum above the knee voltage, avoiding the non-linear current waveform modulation.

As long as the designer avoids the clipping region of the smith chart, the voltage waveform will avoid the knee region and the current waveform will not be modulated. Once the voltage waveform begins to distort the current waveform, efficient and linear operation can no longer be guaranteed.

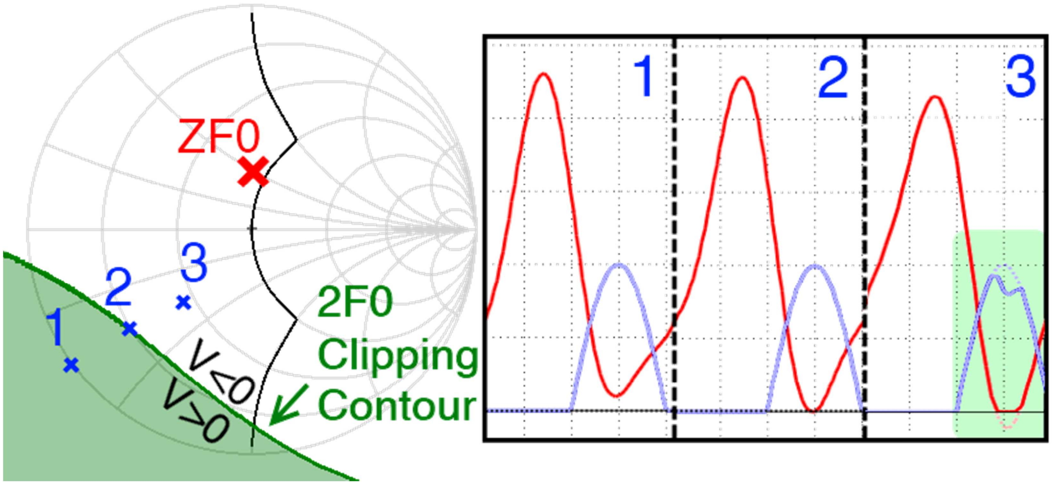

Figure 3: Demonstrating that clipping contours represent the "zero grazing" boundary (v1r=0.9, v1q=0.5).

Figure 3 demonstrates a clipping contour drawn for an arbitrary ZF0, one which belongs neither to a classical mode, nor to the continuous design space (which stipulate v1r must always equal unity). Clipping contours are in fact **valid for any ZF0**, and will show all valid Z2F0 zero grazing impedances, if any exist. The numbered Z2F0 points shown in Figure 3 correspond to waveforms shown on the right hand side. From this it can clearly be seen that the clipping contour represents the “zero grazing case”.

Figure 3 also demonstrates how a reduction in v1r allows the device to absorb a non-zero v2r without producing a voltage waveform which will modulate the current waveform. Importantly, the expanded clipping region also shows a large degree of **reactive freedom**, proving the v2q/v1q relationship described in Class B/J theory, is in practice very forgiving, and need not be rigidly adhered to.

It is important to note once more, that as the Fourier coefficients (2) were normalised to DC, v1r and hence the real part of ZF0 are the sole determinant of both power and η. All Z2F0 impedances both on the clipping contour and inside the clipping region correspond to identical power and η values.

10W GALLIUM NITRIDE DESIGN

Using a Cree CGH40010F 10W Gallium Nitride device, an RFPA was designed to demonstrate the use of the clipping contour tool. The circuit initially targeted a fundamental band of 2-3GHz and was tuned to optimize ZF0 whilst minimising the real part of Z2F0. The reactance ratio between fundamental and second harmonic, as specified by classical Class B/J theory, was relaxed to achieve minimal real Z2F0, shown in Figure 3 to be more important in avoiding clipping the current waveform.

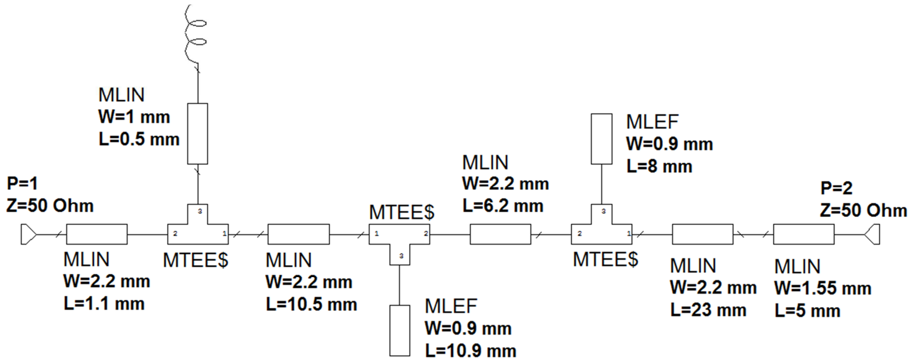

Figure 4: Ideal output matching circuit (device drain at port 1).

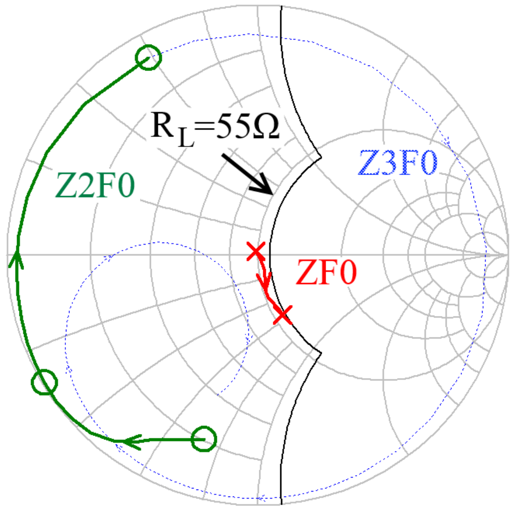

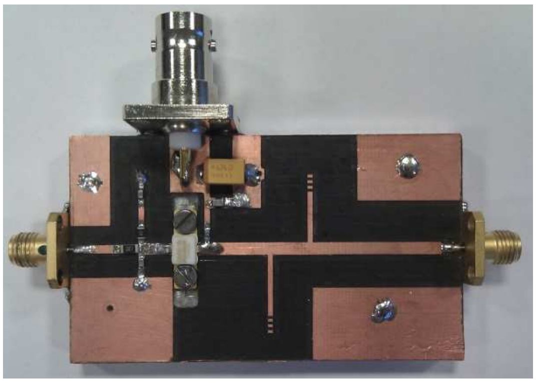

Figure 5: Matching impedances at the Igen plane showing ZF0 from 2-3GHz and Z2F0 from 4-6GHz.

S parameters of the packaged and unpackaged die were freely available from the device manufacturer. Converting to ABCD matrices and applying simple matrix manipulation, S parameters blocks for the package parasitics were extracted. The final deembedding step involved the use of an ideal inductance to model the internal bond wire, a wide section of transmission line to model the bonding pad and an ideal capacitance to model the device drain source parasitic capacitance.

While this simple technique proved acceptable at the low GHz frequencies targeted by this design, the degree of error will be unacceptable at higher frequencies. Ideally, the cold FET parasitic extraction technique would be used to model the parasitics. The lack of an available device fixture prohibited use of this technique.

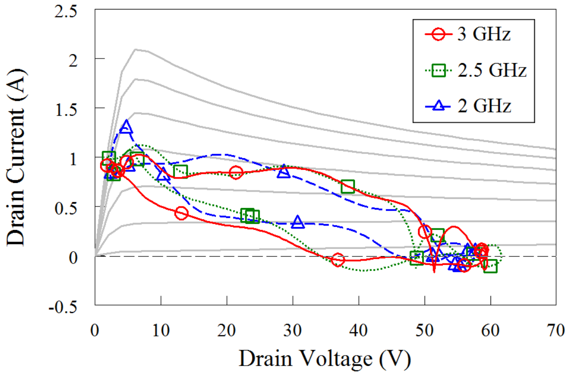

Figure 6: Simulated Dynamic load lines showing the Igen waveform shapes across the operating band overlain on the simulated DCIV traces of the CGH40010F. Drive power was 29dBm.

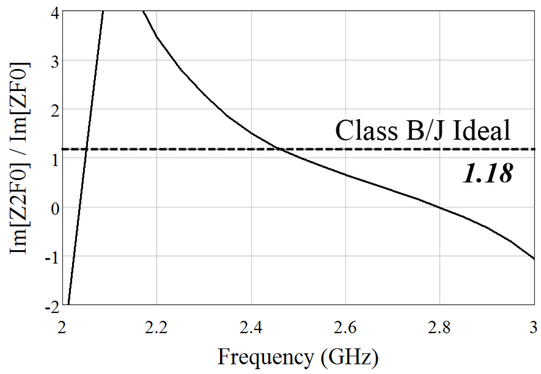

Figure 7: Simulated ratio of Z2F0/ZF0 reactance, showing the ideal Class B/J value overlain.

A commercially available large signal device model provided by Cree was used to verify the simple deembedding network (Figure 6) by verifying the load line stayed within the device operating boundaries.

As previously stated, clipping contours predict a large degree of flexibility in the Z2F0/ZF0 reactance ratio. Figure 7 shows how this ratio was allowed to vary over the targeted fundamental frequency range, compared with the ideal Class B/J ratio of 1.18.

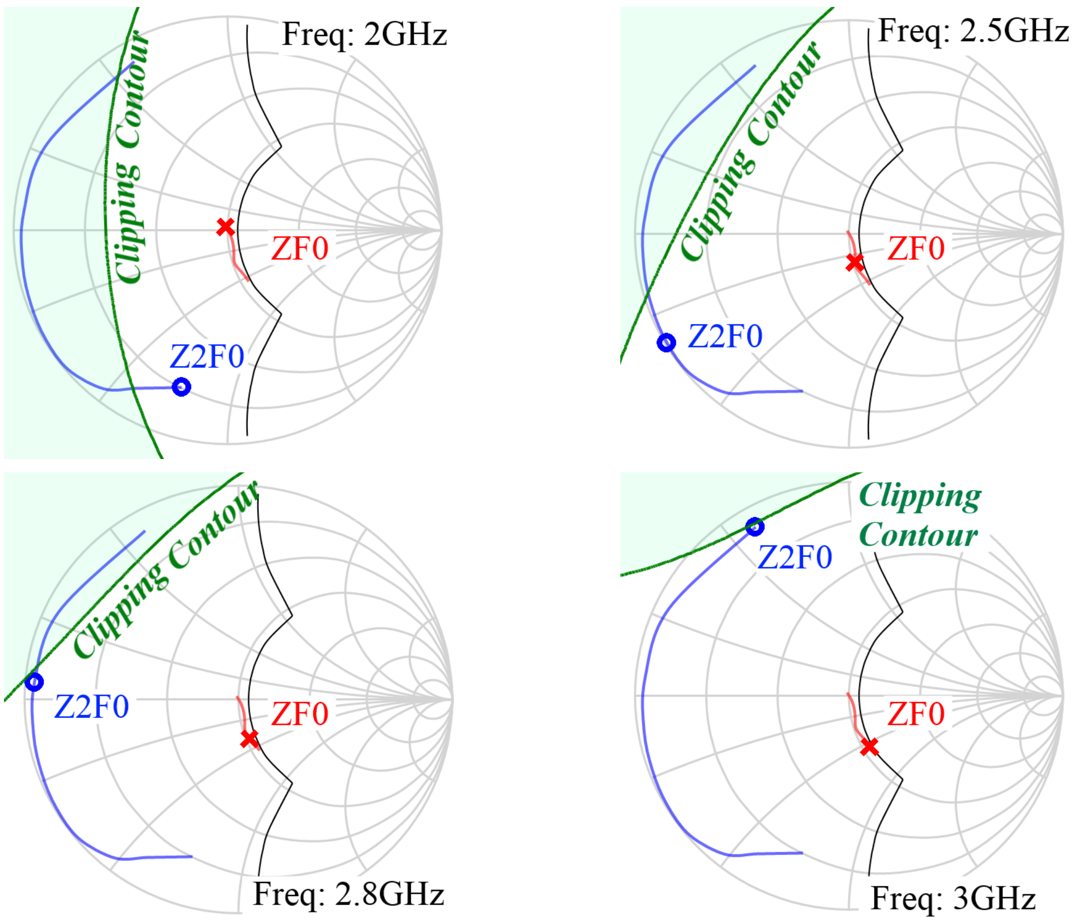

Figure 8: The clipping contours calculated over frequency from the simulated output matching networks Igen impedances.

Key to the design of this network was the second harmonic clipping contour tool. Variation in Z2F0/ZF0 reactance was permitted to the extent that the clipping contour condition was not *strongly* violated. The design targeted high η, thus some violation of the clipping contour was deemed acceptable. Figure 8 shows that a small reduction in fundamental impedance (compared to the predicted RL) produced enough design space at the second harmonic to allow the circuit to follow the clipping contour over the original design bandwidth.

The circuit was fabricated at Cardiff University using a Rogers Corporation RT5880 duriod substrate (508mm thick) with a thick clad aluminum back coating for physical robustness and optimal thermal performance. The output matching network avoided the use of external capacitors to maximize the circuit Q and attempt to reduce fabrication variation due to human error.

MEASURED RESULTS

All of the following results are measured with an input power of 29dBm, a drain voltage of 28V and a gate voltage of -2.8V.

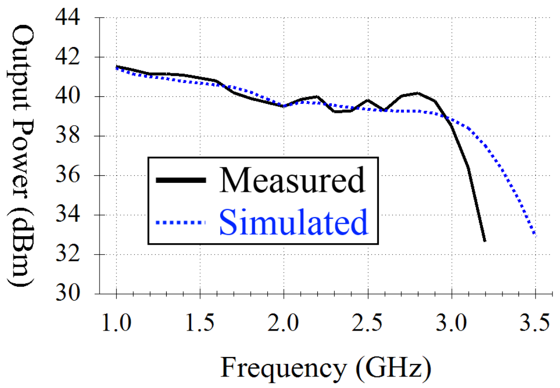

Figure 9: Measured output power versus frequency for a constant input power (29dBm).

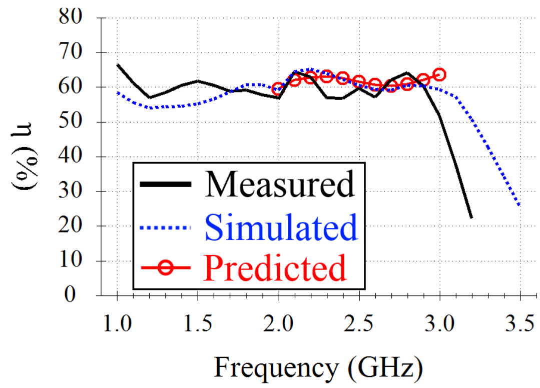

Figure 10: Measured η versus frequency for a constant input power (29dBm).

The circuit achieved at least 8.5W output power over the whole of the design band and a maximum output power of 10.4W at 2.8GHz (Figure 9). The power appeared to roll off above 2.9GHz. The performance extended well below the design band, suggesting the efficacy of the selected low pass topology.

Drain efficiency (Figure 10) followed the trend of output power, with a nominal value of 60% from 1-2.9GHz. The predicted value shown in Figure 10 was calculated using an extremely simple knee model (4).

$$I_k(\theta) = I(\theta)\log_2\left(\frac{V(\theta)}{Vknee} + 1\right)^{0.71} \qquad \textbf{(4)}$$

This knee model was applied to the current waveform if the clipping contours algorithm predicted the voltage would clip the current. Both waveforms were then passed through the Fourier transform and the efficiency was calculated. This result demonstrates once more the power of the clipping contour tool and the importance of avoiding major current waveform modulation in achieving high efficiency operation.

Previous work has shown this device capable of up to 70% η under certain conditions. The design was conservative with the selection of RL to expand the clipping contour design space, thus limiting the efficiency that could be achieved. A higher value of RL would generate less output power because of the lower Imax, but would enable a lower minimum voltage and correspondingly a higher efficiency at the expense of gain. This highlights the importance of choosing an appropriate RL value to achieve optimal performance.

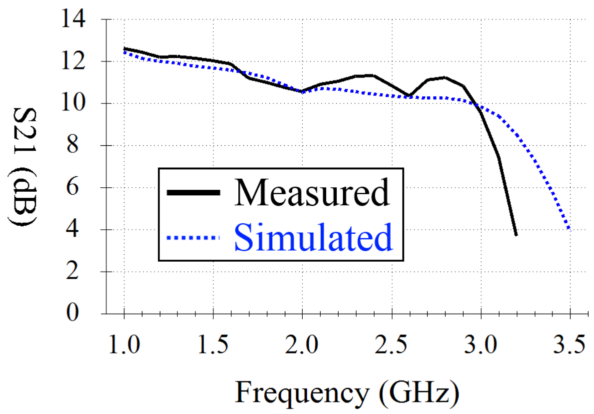

Figure 11: S21 at a constant input power (29dBm).

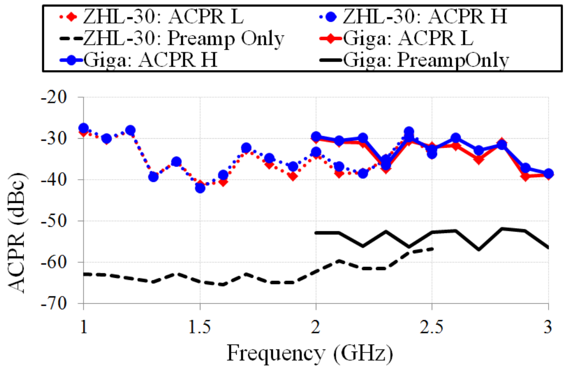

Figure 12: Measured ACPR with single carrier WCDMA at a constant input power (29dBm). No attempt has been made to linearize the circuit.

Large signal gain is also high for the device (Figure 11), an advantage of operating in a, nominally, uncompressed mode.

Figure 12 demonstrates a representative linearity measurement with a 5MHz single carrier WCDMA signal (3.84 chips/s, 0.22 raised root cosine filter). The presented numbers are raw figures from the device without any attempt at linearization. The amplifier shows a nominal ACPR 30dB below the carrier frequency from 1-3GHz.

Due to the wide bandwidth of the device, two separate pre-amplifiers were necessary, Preamplifier A was used to measure 1-2.5GHZ and Preamplifier B above 2.5GHz. Figure 12 shows separate traces for each of the pre-amplifiers. Preamplifier B degraded the signal slightly more than the Preamplifier A, consequently the true linearity figure of the clipping contours amplifier may be lower.

CONCLUSION

The power of clipping contours, especially their role in identifying RFPA operating mode sensitivity to impedance mismatch, has been demonstrated. An example RFPA was designed, fabricated and measured, showning how second harmonic clipping contours can be integrated into a traditional design flow targeting high η and linearity over broad bandwidths.

The non clipping contour violating circuit was capable of at least 8.5W from 1-2.9GHz and 9W from 1-2.2GHz and 2.7-2.9GHz. The measured η was approximately 60% from 1-2.9GHz with a minimum value of 56.8% at 2GHz. The unpredistorted linearity was tested under single carrier WCDMA and achieved an ACPR of at least -30dBc from 1-2.9GHz.

The clipping demonstrator exhibited performance degradation closely correlated to the extent the clipping contour condition was violated.

ACKNOWLEDGEMENTS

The authors would like to thank Angus McLachlan from Selex Galileo Edinburgh for advice and support and Cree Semiconductor for supplying the transistors.

REFERENCES

[1] F. Raab, “Class-F power amplifiers with maximally flat waveforms,” IEEE Transactions on Microwave Theory and Techniques, vol. 45, no. 11, pp. 2007 –2012, Nov 1997.

[2] F. Giannini and L. Scucchia, “A Complete Class of Harmonic Matching Networks: Synthesis and Application,” Microwave Theory and Techniques, IEEE Transactions on, vol. 57, no. 3, pp. 612 – 619, march 2009.

[3] N. Sokal and A. Sokal, “Class E-A new class of high-efficiency tuned single-ended switching power amplifiers,” Solid-State Circuits, IEEE Journal of, vol. 10, no. 3, pp. 168 – 176, jun 1975.

[4] J. Everard and A. King, “Broadband power efficient Class E amplifiers with a non-linear CAD model of the active MOS device,” Electronic and Radio Engineers, Journal of the Institution of, vol. 57, no. 2, pp. 52 –58, march-april 1987.

[5] K. Chen and D. Peroulis, “Design of Highly Efficient Broadband Class-E Power Amplifier Using Synthesized Low-Pass Matching Networks,” Microwave Theory and Techniques, IEEE Transactions on, vol. 59, no. 12, pp. 3162 –3173, Dec. 2011.

[6] J. D. Rhodes, “Output universality in maximum efficiency linear power amplifiers,” International Journal of Circuit Theory and Applications, vol. 31, no. 4, pp. 385–405, 2003.

[7] S. Cripps, P. Tasker, A. Clarke, J. Lees, and J. Benedikt, “On the Continuity of High Efficiency Modes in Linear RF Power Amplifiers,” Microwave and Wireless Components Letters, IEEE, vol. 19, no. 10, pp. 665 –667, Oct. 2009.

[8] P. Wright, J. Lees, J. Benedikt, P. Tasker, and S. Cripps, “A Methodology for Realizing High Efficiency Class-J in a Linear and Broadband PA,” Microwave Theory and Techniques, IEEE Transactions on, vol. 57, no. 12, pp. 3196 –3204, Dec. 2009.

[9] V. Carrubba, A. Clarke, M. Akmal, J. Lees, J. Benedikt, P. Tasker, and S. Cripps, “The Continuous Class-F Mode Power Amplifier,” Microwave Integrated Circuits Conference (EuMIC), 2010 European, pp. 432 –435, Sept. 2010.

[10] J. Powell, M. Uren, T. Martin, A. McLachlan, P. Tasker, S. Woodington, J. Bell, R. Saini, J. Benedikt, and S. Cripps, “GaAs X-band high efficiency (>65%) Broadband (>30%) amplifier MMIC based on the Class B to Class J continuum,” in Microwave Symposium Digest (MTT), 2011 IEEE MTT-S International, June 2011, pp. 1 –4.

[11] V. Carrubba, A. Clarke, M. Akmal, J. Lees, J. Benedikt, P. Tasker, and S. Cripps, “On the Extension of the Continuous Class-F Mode Power Amplifier,” Microwave Theory and Techniques, IEEE Transactions on, vol. 59, no. 5, pp. 1294 –1303, May 2011.

[12] Canning, T. and Tasker, P. and Cripps, S., “Load Pull verification of a novel Class B/J design tool: Second Harmonic Clipping Contours,” in Microwave Measurement Symposium (ARFTG), 2013 81th ARFTG.

[13] S. C. Cripps, RF power amplifers for wireless communication, 2nd ed. Norwell, MA: Artech House, 2006.

[14] Canning, T.; Tasker, P.; Cripps, S., "Waveform Evidence of Gate Harmonic Short Circuit Benefits for High Efficiency X-Band Power Amplifiers," *Microwave and Wireless Components Letters, IEEE* , vol.23, no.8, pp.439,441, Aug. 2013